

Research Article

The Evaporation Behavior of Volatile Fission Products in FLiNaK Salt

Masami Taira¹, Yuji Arita², and Michio Yamawaki²

¹*Advanced Interdisciplinary Science and Technology, Graduate School of Engineering, University of Fukui, Kanawa-cho,1-2-4, Tsuruga, Fukui, Japan*

²*Research Institute of Nuclear Engineering, University of Fukui, Kanawa-cho,1-2-4, Tsuruga, Fukui, Japan*

Abstract. Molten salt reactor (MSR) was suggested for the one of the nuclear power plant concepts planned for generation IV. However, little study had been done on the severe accident at MSR. The one of the severe accident at MSR is considered that the molten salt with fuel will be exposed to air and some fission products will release to environment. The molten FLiNaK salt (LiF-NaF-KF: 46.5–11.5–42 mol%) with CsI(FLiNaK- CsI : 99-1 mol%) was evaporated and released gases were measured by mass spectrometry. The evaporated gases from above sample were mainly CsI and KI. The value of vapor pressure for CsI was low about ten to the first ~ second power of vapor pressure for pure CsI at same temperature. Therefore, it is expected that FLiNaK prevents the release of CsI. On the other hand, despite KI were not included in original sample, KI released significantly.

Keywords: molten salt, cesium iodide, vapor pressure, quadrupole mass spectrometry

Corresponding Author

Masami Taira
masami_taira@yahoo.co.jp

Editor

Luigi Rodino

Dates

Received 10 October 2017
Accepted 11 October 2017

Copyright © 2017 Masami Taira et al. This is an open access article distributed under the Creative Commons Attribution License, which permits unrestricted use, distribution, and reproduction in any medium, provided the original work is properly cited.

1. Introduction

Molten salt reactor (MSR) is one of the nuclear power plant concepts planned for Generation IV systems [1]. The schematic illustration of typical MSR shows as Figure 1. MSR were first developed in the Oak Ridge National Laboratory (ORNL), United States in around 1950s to 1970s. In this term, the experimental reactor was constructed and operated [2, 3]. However, the MSRs project was frustrated due to several issues [3, 4]. In 2000's, improved MSR was chosen for the one of the next-generation reactors in the Generation IV International Forum [1]. The most interesting point about MSRs is that the nuclear fuel was dissolved into molten salt of primary loop, and the molten salt served as coolant. The fissile elements which were dissolved in molten salt will fission at the core. The core is covered by neutron moderator or neutron reflector, therefore the nuclear fission is occurred at only the core. The heat generated by nuclear fission will be transported by primary molten salt. At heat exchanger, this heat is transported to the secondary loop, in which the molten salt of second loop doesn't contain fissile elements-. Finally, this heat makes steam and converted to electricity.

There are critical issues for nuclear power plant; i.e. how to treat the transuranium elements (TRU) and long-half-life fission products (LLFP). MSRs can be able to solve these issued because MSR can customize to use fast neutron spectrum, as the transmutation of TRU LLFP. For transmutation of TRU, a molten salt fast reactor (MSFR)—or fast spectrum molten salt reactor (FS-MSR)—is the candidate reactor [5–7]. On the other hand, MSR is one of candidate reactor for using of thorium for fuel since thorium captures thermal or fast neutron to generate



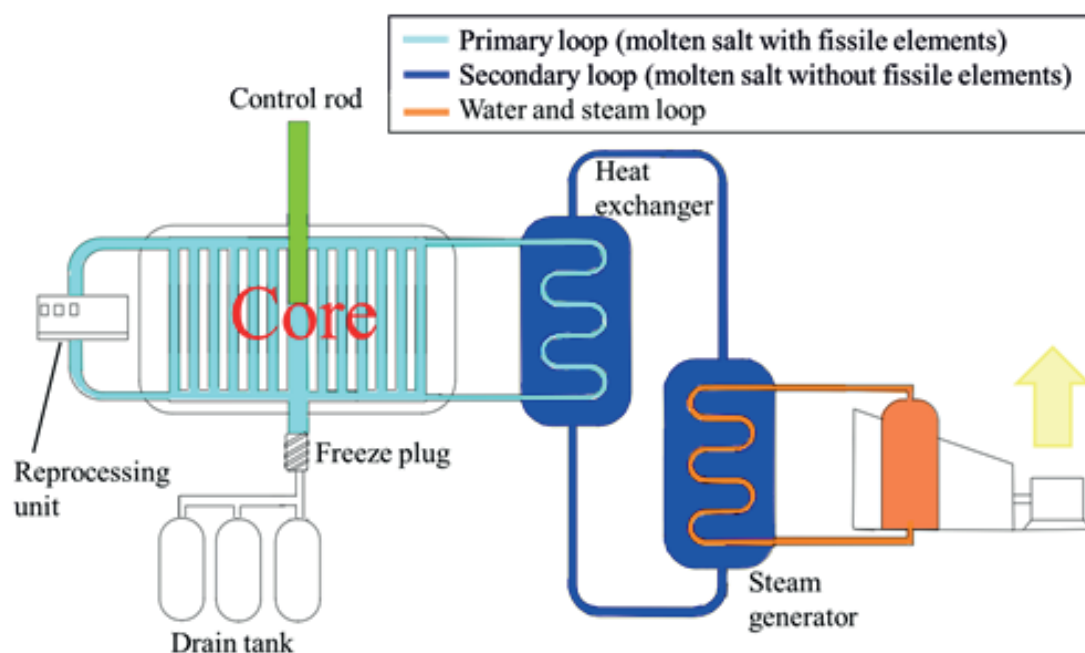


Figure 1: Schematic illustration for MSRs.

Th-233 which decay to U-233 (and it is fissionable element) and thorium can dissolve to molten salt. A thorium molten salt reactor (TMSR) has been studied for fuel breeding using thorium elements [7]. Recently, the MSRs in combination with fast spectrum and using thorium was suggested [5]. There are several types of MSRs and Table 1 lists major MSRs [5, 8]. Moreover, the one of MSR's advantage is that reprocessing unit for fuel salt can be connected to primary loop [9]. It enables to reprocessing fuel salt with online and continue the plant operation, further the construction of reprocessing plant don't need in other place, also transport of fuel salt to reprocessing plant don't need. Therefore, production of solid fuel consists TRU doesn't need, only need process is dissolving TRU to fuel salt at reprocessing unit on MSRs. In summary, MSRs have some potential for using the thorium, transformation TRU or LLFP (for only fast spectrum), and it is expected that there is no need to transform the spent fuel salt to other place for reprocessing or re-product the TRU fuel.

However, MSRs had been constructed only one time moreover it is experimental reactor (molten salt reactor experiment—MSRE—on 1960's by ORNL), therefore some issue should be clear for construction of MSRs in future. They are the corrosion of construction material with molten salt, the radiation caused by thorium - uranium cycle, to clear the regulation for acceptance from regulatory agency (like IAEA or NRC), and clarify the behavior when severe accident (SA) happened.

The concept of Generation IV was defined as using fuel more efficiently, reducing waste production, being economically competitive, and meet stringent standards of safety and proliferation resistance [1]. For MSRs, it considers that if the loss of cooling activity happened and fuel salt was heated, the freeze plug which is made of same salt of primary loop will melt and fuel salt will drop to drain tank (Figure 1). This tank is designed to prevent the critical state of fuel salt. Hence, it was expected that the events leading to severe accidents at light water reactor

(LWR) don't need to consider for MSR. However, many term can be consider to cause SA and it need to take some measures for SA. The one of the guessable SA is that the pipe of primary loop will be fractured, then the molten salt with fuel will exposed to air and FPs will release to environment. The environment pollution which causes by the release of FPs is one of the important issues. To appraise the safety of MSRs during SA, it is vital to understand the release behavior of radioactive FPs.

Table 1: Molten salt reactor concept description (Ac means actinides, HN means heavy nuclides).

Comcept	Feed	Molten salt (mol%)	Neutronic spectrum	Reprocessing	Reactivity	Ref.
TIER	TRU	NaF-ZrF ₄ (80-20)	Thermal (graphite moderator)	No	Subcritical ADS use	[20, 21]
SPHINX (Czech Republic, Nuclear Research Institute Rez plc)	TRU	LiF-NaF-BeF ₂ (35-27-38)	Fast (graphite used as reflector)	Yes	Critical	[22, 23]
MOSART (Russia, Kurchatov Institute of Russia)	TRU 2-3mol%	LiF-NaF-BeF ₂ (15-58-27)	Fast (graphite used as reflector)	No	Critical	[24, 25]
Critical MSR	TRU	LiF-NaF-BeF ₂ (15-58-27)	Fast (no graphite used)	Yes (FP extraction unit)	Critical	[26]
JAERI MSR	TRU	NaCl-AnCl ₃ (64-36)	Fast (chloride media)	No	Subcritical	[27, 28]
TASSE	ThF ₄ No fissile (TRU in the first install-ations)	PbCl ₂ -AnCl ₃ (70-30)	Fast superthermal	Partial recycling, U, Pa, Th, TRU in wastes	Subcritical	[29, 30]
WISE	Natural fuel ²³⁸ U or ²³² Th	Na ³⁷ Cl-Ac ³⁷ Cl ₃ (60-40) Pb ³⁷ Cl ₂ -Ac ³⁷ Cl ₃ (60-40)	Hard fast spectrum	No	Critical with U [31] Subcritical with Th, it needs ADS	
CSMSR		two salts: LiF-BeF ₂ -MF ₃ (M = MA + Pu, Th,U) LiF-BeF ₂ -MF ₃ -XF ₃ (X = Gd, sm) (absorber)			Subcritical	[32]
MSRE	²³⁸ U, ²³⁵ U, ²³³ U after 6 months	LiF-BeF ₂ -ZrF ₄ -UF ₄ (65-29.1-5-0.9)	Thermal	Partial fluorination to recover U	Critical	[33, 34]
Comcept	Feed	Molten salt (mol%)	Neutronic spectrum	Reprocessing	Reactivity	

Concept	Feed	Molten salt (mol%)	Neutronic spectrum	Reprocessing	Reactivity	Ref.
MSBR	^{232}Th ^{233}U	LiF-BeF ₂ -ThF ₄ -UF ₄ (71.6-16-12-0.4)	Thermal graphite moderator and reflector	Yes	Critical	[35, 36]
THORIM-NES FUJI-II (small MSR)	^{232}Th ^{233}U	LiF-BeF ₂	Thermal (graphite moderator and reflector)	Partial He bubbling Filtration of solids formed in the molten salt, redox control	Critical	[37]
THORM-NES AMSB	^{232}Th and/or ^{233}U	Molten salt target Standard: LiF-BeF ₂ -ThF ₄ (64-18-18) or High-gain type: LiF-BeF ₂ -ThF ₄ -UF ₄ (64-18-17.5-0.5)	Thermal graphite blocks immersed in the salt	Partial	Subcritical	[37, 38]
AMSTER (BREEDER)	^{232}Th or ^{238}U and ^{235}U	LiF-BeF ₂ -(HN)F ₄ (61-21-18)	Thermal graphite moderator	Yes fission products extraction and injection of Hn in the salt		[39, 40]
REBUS (France, EDF Research and Development, CEA)	UTR U	(U, TRU) Cl ₃ -NaCl TRU: 15.6 at%	Fast	Yes fission products extraction and depleted U feed	Critical	[41, 42]
MSFR	^{232}Th , ^{233}U	Fertile blanket LiF-ThF ₄ (72-28)	Fast (graphite removal)	Yes	Critical	[43-47]
SMSFR	Th, ^{233}U , MA	FLiNaK-(ThF ₄ + UF ₄ + MAF ₃) (70-30)	Fast	Yes	Critical	[12]

Many salts, such as fluorides and chlorides, can be used as the coolant and solvent salt for fuel [10]. In this experiment, the release behaviors of radioactive FPs from a mixture of LiF-NaF-KF (FLiNaK) molten salt were investigated. FLiNaK is one of the candidates which expected as a coolant or fuel solvent in MSFRs [11]. Primary loop is often used FLiBe (LiF - BeF₂) in many concept, in the other hand some design uses FLiNaK for primary loop [12]. The properties of FLiNaK are indicated in Table 2. The focus of this investigation is the release of the radioactive FPs cesium and iodine, since these were the main factor for environmental pollution in TEPCO's 1F disaster.

Table 2: Basic properties of FLiNaK salt [11].

Eutectic composition (mol %)	LiF-NaF-KF46.5-11.5-42.0
Melting point (K)	727
Density (kg/m ³)*	2579.3-0.6240 T(K)

* Density depends on temperature (T in kelvin)

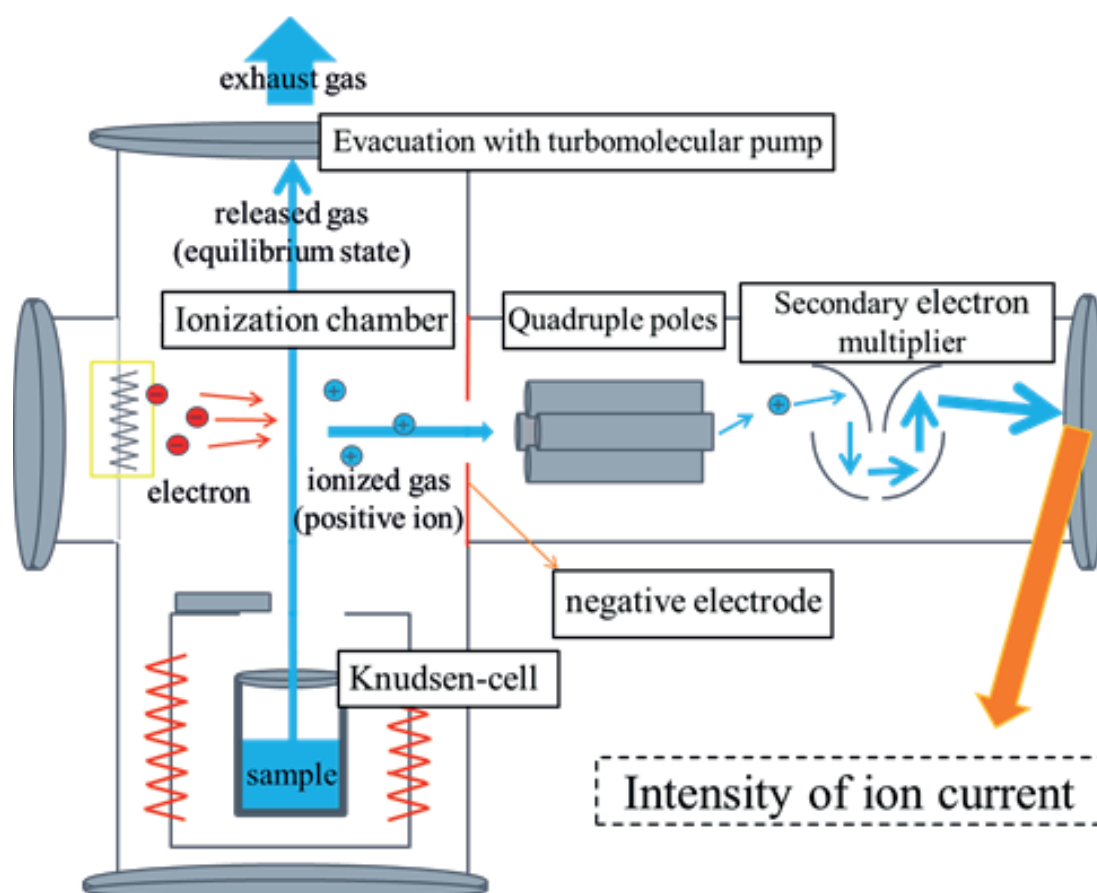


Figure 2: Schematic illustration of equipment.

2. Experiments

Quadrupole mass spectrometer. In this experiment, quadrupole mass spectrometer (QMS) was used for observation of the released gas species. The schematic drawing of QMS is Figure 2. At the First, the Knudsen-cell was heated, then the evaporated gas was released to an ionization chamber. In this chamber, there were many electrons which were generated from filament made of tungsten by heating. Then, evaporated gas was ionized to positive ion by these electrons. Most gas was decomposed by the impact of electron (some gas was ionized keeping the chemical form). This decomposed gas ion will be detected as the result. The positive ion was attracted by the negative electrode and introduced to QMS. Then, specific mass ion can trough these poles. The specific ion collided to secondary electron multiplier, and this signal was amplified. The amplified signal was detected by computer, and this value was detected for “intensity of ion current”.

Vapor pressure measurements. The vapor species from molten salt and their respective vapor pressure were measured using a QMS (Pfeiffer Vacuum GmbH QMG700) with a Knudsen cell [13]. The Knudsen cell was made of nickel, and had an internal diameter of 8 mm and a height of 8 mm. The diameter of the effusion orifice plate was 0.5 mm. The electron energy used to

Table 3: Ionization cross-section, appearance potential and isotope abundance ratio for representative ions.

Vapor gases	Maximum ionization cross section $\sigma(i)$ (10^{-16}cm^2) [48]	Appearance potential (eV)	Isotope abundance ratio S_j
^7Li (g)	3.50	4.73	0.926
^{23}Na (g)	4.27	11.05	1
^{39}K (g)	7.67	6.36	0.931
$^{39}\text{K}^{127}\text{I}$ (g)	14.6	12.26	0.931
^{133}Cs (g)	11.5	11.12	1
^{127}I (g)	6.92	11.86	1
$^{127}\text{I}_2$ (g)	10.4	14.14	1
$^{133}\text{Cs}^{127}\text{I}$ (g)	18.4	8.98	1
$^{133}\text{Cs}_2^{127}\text{I}$ (g)	27.6	8.51	1

ionize the gaseous atom or molecule was 20 eV. The partial pressure $P(i)$ was calculated using equation (1) [14].

$$P(i) = \sum_j k \frac{I_j(i)T}{\gamma_j S_j \sigma(i) \Delta E_j} \quad (1)$$

where k is the proportionality constant and depends on the apparatus condition, j is the target ion for measurement, $I_j(i)$ is the intensity of the current for ions j , T is the temperature of Knudsen cell during measuring, $\sigma(i)$ is the ionization cross-section, γ_j is the isotope abundance ratio for ions j , S_j is the relative multiplier gain of the detector for ions j ($\propto m^{-1/2}$ [15]), and ΔE_j is the difference between the appearance potential for ions j and the electron beam energy for ionizations. The maximum ionization cross-sections, appearance potentials and isotope abundance ratios are listed in Table 3. The ionization cross-sections for monomeric gas species were computed by taking the sum of atomic cross-sections of the component atoms, estimated by Mann [16]. In the case of complex such as K_2F and KCsF , these data were calculated as 0.75 times the sum of the cross-section for monomers, as proposed by Miller [17, 18]. The ionization efficiency curves for each species were obtained for ionization energies from 1 to 22 eV. Some alkali metal ions were able to detect at two range of ionization energy -about 1eV and 20eV-. In the range of low ionization energy -around 1eV-, some alkali metal ions were able to detected, however iodine and cesium iodide were not able to be detected. Therefore, we had chosen the ionization energy to 20eV. By linear extrapolation of the ionization efficiency curves to zero intensity, the appearance potentials of gas species were determined, as shown in Table 3.

The proportionality constant “ k ” was obtained from the comparison of the $p(\text{CsI})^2/p(\text{Cs}_2\text{I}_2)$ ratio with reported equilibrium constant for $2\text{CsI}(\text{g})=\text{Cs}_2\text{I}_2(\text{g})$ from thermodynamic database as equation (2) [12, 14].

$$\frac{p(\text{CsI})^2}{p(\text{Cs}_2\text{I}_2)} = \frac{k^2}{k} \cdot \frac{p(\text{CsI})^2/k^2}{p(\text{Cs}_2\text{I}_2)/k} = k \cdot \frac{p(\text{CsI})^2/k^2}{p(\text{Cs}_2\text{I}_2)/k} = K_p = A \cdot \exp(-B \cdot T^{-1}) \quad (2)$$

where $p(\text{CsI})$ and $p(\text{Cs}_2\text{I}_2)$ are vapor pressure of CsI and Cs_2I_2 , respectively. A and B are constant. A and B are different between each measurement.

Table 4: Concentration ratio for samples.

Sample name	FLiNaK [mol%]	CsI [mol%]
CsI-0%	100	0
CsI-1%	99	1
CsI-10%	90	10
CsI-25%	75	25
CsI-50%	50	50
CsI-100%	0	100

In this study, the value of $p(\text{CsI})^2/k^2$ and $p(\text{Cs}_2\text{I}_2)/k$ were obtained from measurement, therefore k was calculated. After the obtained k from data at until 973K was plotted, the A and B were driven by equation (2). The reason to use the value k from at until 973K is that CsI started to evaporate significantly at over 973K. Therefore the k was calculated from equation (2) and this k was used for at high temperature.

It expected that the calculated k contains inaccuracy. Generally, mass spectrometry is difficult to determine the absolute value of vapor pressure for quantitative analysis. The result of this study should be considered for understanding the trend when FLiNaK-CsI evaporated.

This experiment used the step wise manner. Targeted temperature was 823, 873, 923, 973, 1023, 1073 and 1173K. After increasing to targeted temperature, it was keeping to stabilize for 5 minutes. Measurement time took 6 minutes (the scan speed was 1sec/ u, and scan range was 360 u. Which u is unified atomic mass unit). The loss time (to save the measurement data and wrote the condition to notebook) might be 1minute. Therefore the total time for measurement was 12 minutes for each temperature.

2.1. Sample preparations

The anhydrous salts eutectic FLiNaK and CsI - typical volatile FP elements - were used for this study. FLiNaK was purchased from APL Engineered Materials Inc., and CsI was purchased from Kojundo Chemical Laboratory Co., Ltd. The both purities were 99.9%. The impurities in each reagent were less than 30 ppm on mill test certificate. However, H₂O (moisture) had not written, therefore some moisture might contaminated. The way to remove the moisture is keeping the temperature of Knudsen cell at about 473K for 24 hours since this temperature is quite high than the boiling point for H₂O, moreover FLiNaK and CsI don't melt.).

Six samples with different concentration of CsI were prepared to measure. The quantity of FP depends on the burnup of nuclear fuel. Generally, CsI was 1 mol% in LWR's fuel. In this study, it is assumed that the inventory of CsI was 1 mol% against FLiNaK. Other samples were changed the CsI concentration ratio for reference samples. The detailed information listed in Table 4.

3. Results and Discussion

In order to confirm which types of gas species evaporate, the vapor from “CsI-0%” and “CsI-50%” was measured at 1284K and 1018K, respectively. As explained above paragraph, evaporated gas was detected by positive ion. At 1018K, the ionic intensity were very weak for “CsI-0%”. It means that FLiNaK is difficult to be evaporated because of stable salt, thus the measuring temperature was decided to 1284K. The result was shown in Figure 3 and it shows that the principle peak were K^+ , Li^+ , Na^+ . It is considered that detected K^+ , Li^+ , Na^+ were generated from KF, LiF, NaF gases by electron impact for ionization as the preliminary experiment for pure KF, LiF, NaF, respectively. H_2O^+ , N_2^+ , CO_2^+ are residual gasses and Zn^+ was detected as the internal standard. In addition, some compound ion, e.g. K_2F^+ , $LiNa_2K_2F_4^+$, $Na_3K_3F_5^+$, were detected, however these ionic intensities were very weak. In this result, it is considered that the evaporated gases were mainly KF, NaF, LiF and some gases formed multimeric gases. The result of “CsI-50%” was shown in Figure 4. For “CsI-50%”, Cs^+ , I^+ , CsI^+ , KI^+ , I_2^+ were detected in addition to K^+ , Na^+ , and Li^+ . It is expected that Cs^+ was generated from CsI gas by electron impact for ionization, and CsI^+ was generated by same mechanism. Likewise, KI^+ was generated from KI gas, and I^+ was generated by KI and CsI gas. K^+ was generated by KI and KF. Na^+ and Li^+ were generated by NaF and LiF, respectively. I_2^+ ion was expected to be generated by combination with decomposed two I ions. It notes that KI^+ was detected. It is expected that KI was generated by the reaction with FLiNaK and CsI. In the previous studies, when the severe accident in the LWR occurred, it is considered that iodine element will mostly combine with Cs element and they release as CsI [19]. It is expected that the generation of KI gas is one of the characteristic points for SA in MSR. Other some complex ions were detected. Comparing with the case of “CsI-0%”, they were different ions. However these intensities were weak and not detected sufficiently. In the result, the mainly evaporated gases from FLiNaK with CsI were CsI, KI, and followed to NaF, LiF.

The next step, the temperature dependence of the predominant vapor species was confirmed. Using the data of detected ionic intensities, the partial pressure “P(i)” was calculated from equation (1) for each ion. For the representative example, the two figures, the case of “CsI-50%” and “CsI-1%”, show in Figure 5 and Figure 6, respectively. These figures show the P(i) of several gas species as a function of temperature. For “CsI-50%”, the highest P(i) was CsI (the sum of vapor pressure for Cs^+ and CsI^+), followed by KI and KF (focused on K^+), and then KI and CsI (focused on I^+). Hereafter the sum of vapor pressure for Cs^+ and CsI^+ was written to P(CsI), P(i) focused on K^+ was written to P(K^+), P(i) focused on I^+ was written to P(I^+). P(i) focused on KI^+ , Na^+ , Li^+ were written to P(KI), P(NaF), P(LiF), respectively. Above 1173K, the P(CsI), P(K^+), P(I^+) were decrease, on the other hand P(NaF) and P(LiF) were increased. It is considered that CsI started to deplete at around 1073K and FLiNaK continued to evaporate at 1173K. The same trend was seen for “CsI-10%” and “CsI-25%”. These results expect that the compound of Cs and K evaporate with temperature, moreover CsI started to deplete over 1073K. The generated K^+ was discussed in the next paragraph. By constant, for “CsI-1%” as seen in Figure 6, the P(i) of P(CsI), P(I^+) were reduced compare with the result of other samples. It notes that Cs^+ , I^+ ion were not decreased at 1173K. It expects that CsI did not deplete at 1173K.

In order to determine the composition dependence of the P(i), the P(i) was plotted against CsI content, as seen in Figure 7 and Figure 8. In the figures for P(CsI), and P(I^+), the P(i) for

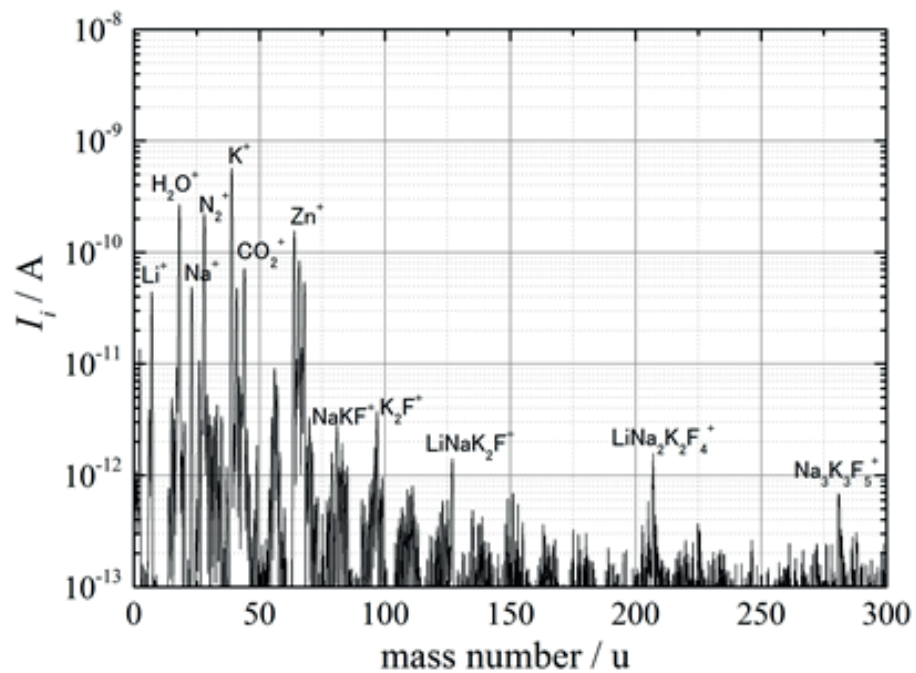


Figure 3: Gaseous ion species from “CsI-0%”.

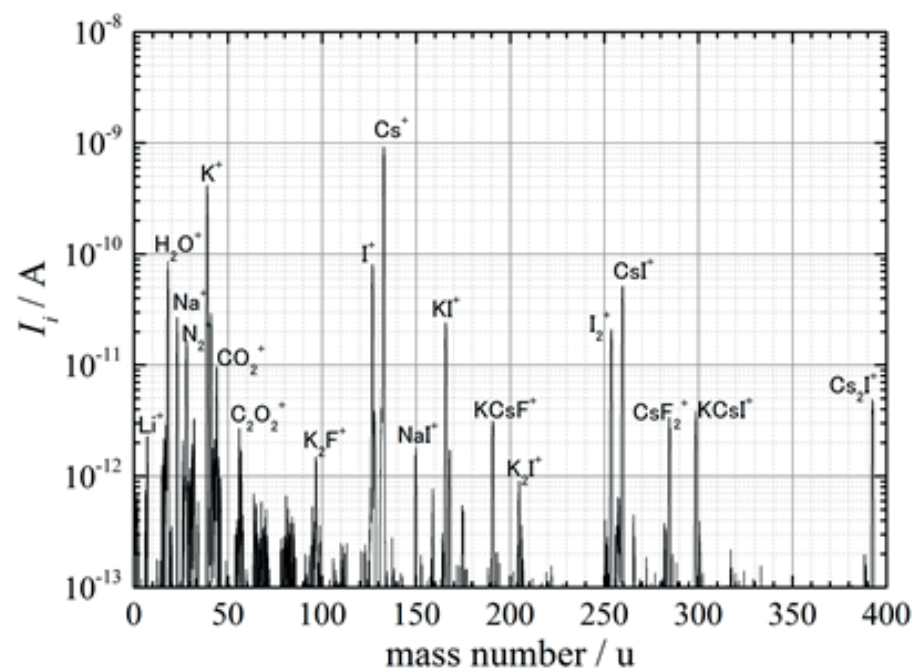


Figure 4: Gaseous ion species from “CsI-50%”.

each sample are shown with the $P(i)$ for “CsI-100%” at 873K to 973K. Because CsI evaporated quickly over 973K, it is difficult to measure $P(i)$ over 1023K for “CsI=100%”.

As shown in Figure 7 and Figure 8, it seems that there are weak dependence on the CsI composition for “CsI=10%”, “CsI=25%” and “CsI=50%”. Moreover $P(\text{CsI})$ was corresponding

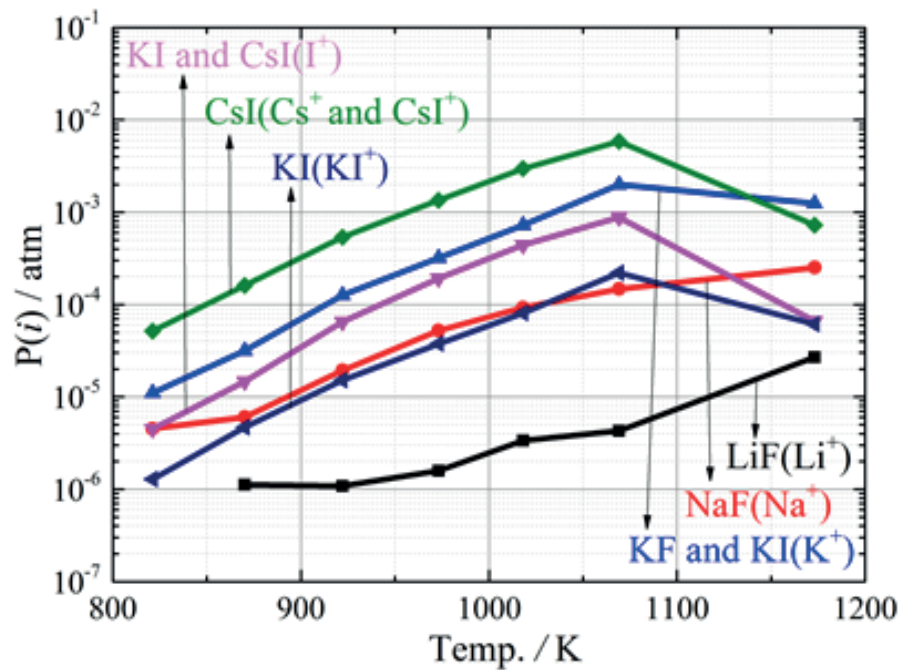


Figure 5: Temperature dependence of $P(i)$ for “CsI-50%”.

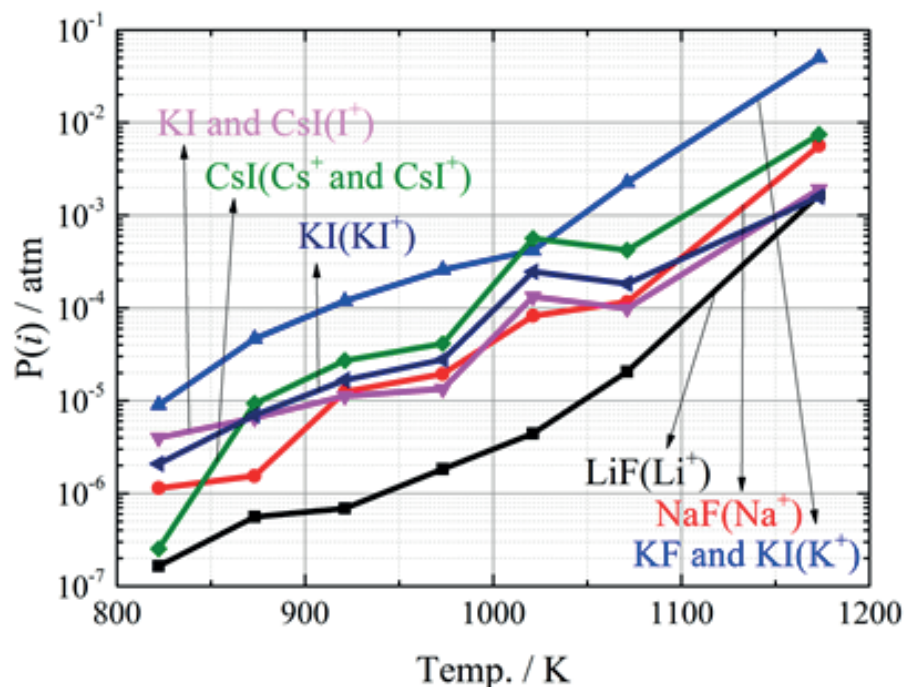


Figure 6: Temperature dependence of $P(i)$ for “CsI-1%”.

with $P(\text{CsI})$ for “CsI=100%”. It is expected that CsI might not be dissolved completely in FLiNaK salt. It is expected that the undissolved CsI might evaporated together with FLiNaK-CsI. Subsequently, $P(\text{CsI})$ of each ion decreased at 1173K. It explained that CsI depleted until 1173K. On the other hand, $P(\text{NaF})$ and $P(\text{LiF})$ were increased. This data might indicate that FLiNaK continued to evaporate at 1173K.

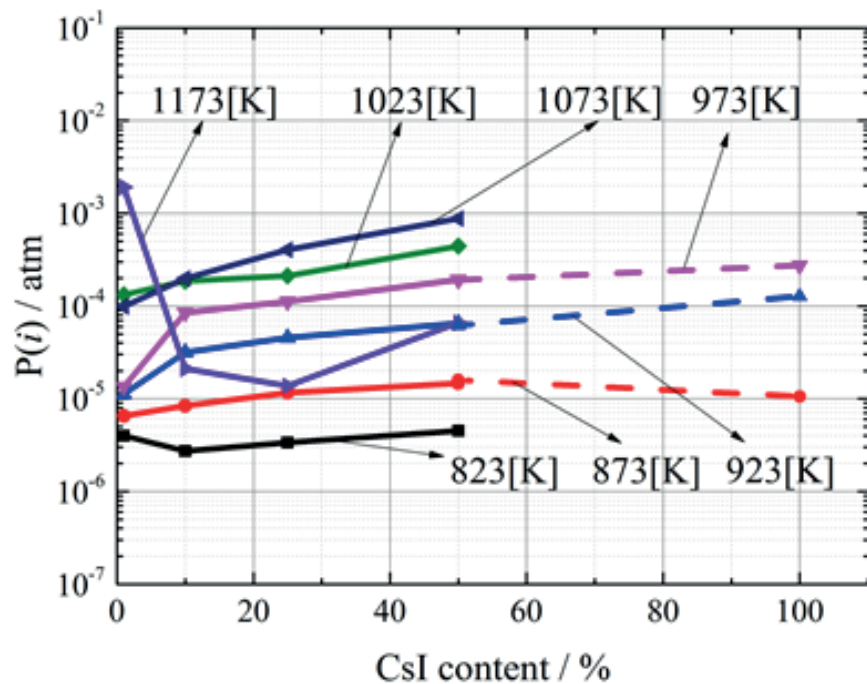


Figure 7: CsI concentration dependence of $P(i)$ for KI and CsI (focused on I^+).

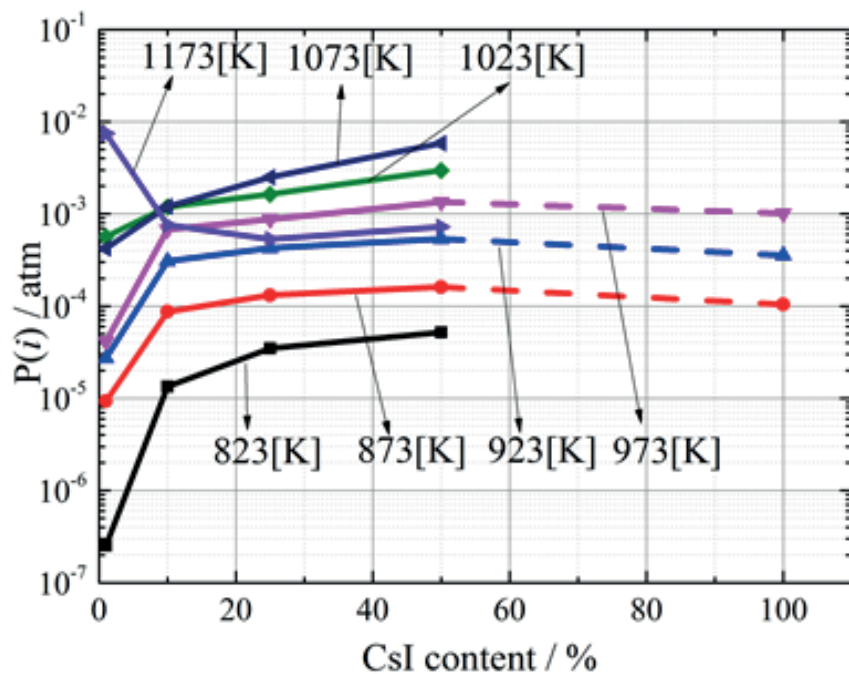


Figure 8: CsI concentration dependence of $P(i)$ for CsI (focused on the sum of Cs^+ and CsI^+).

In the case of “CsI-1%”, $P(CsI)$ was low about ten to the first ~ second power of the $P(CsI)$ value for “CsI=100%”. Similarly, $P(I^+)$ for “CsI-1%” was low about ten to the first ~ second power of that $P(I^+)$ for the “CsI=100%”. It expects that the FLiNaK media suppresses the evaporation of CsI. However, $P(CsI)$ was increased significantly at 1023K to 1073K, and these values are near to the $P(CsI)$ value in the case of “CsI=100” at 973K. Figure 9 makes simple to compare with $P(CsI)$. This figure plotted the $P(CsI)$ for each sample and $P(CsI)$ of CsI gas

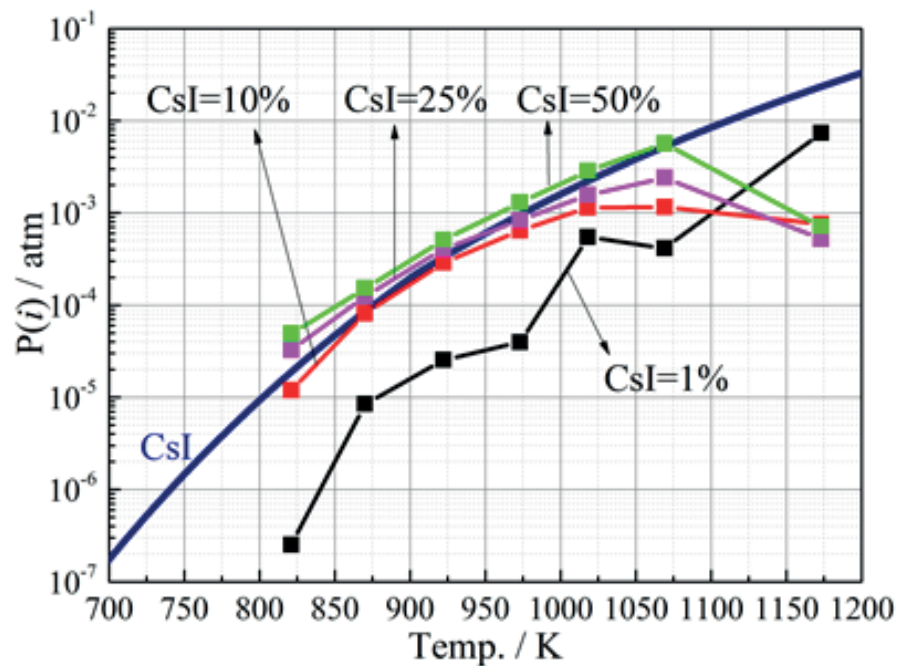


Figure 9: Comparing the thermodynamic database for CsI, and $P(i)$ of CsI (focused on the sum of Cs^+ and CsI^+) for each samples.

from thermodynamic data. On average, each $P(\text{CsI})$ for “CsI-1%” was low about ten to the first ~ second power of that $P(\text{CsI})$ of CsI gas from thermodynamic data from this figure.

In the results, it is expected that if severe accident occurred in MSR, the release quantity of CsI will have the margin of temperature about 100K than the case of LWR. However if the temperature of FLiNaK-CsI will be over 1073K, CsI is considered to release significantly because CsI will start to evaporate quickly at over 973K.

Figure 10 shows the CsI concentration dependence of $P(\text{KI})$. This vapor species is another type of compounds including I element and may affect the radioactive FP release from molten salts. It is expected that KI generated with the reaction between FLiNaK and CsI. It is expected that the quantity of generated KI gas depends on the quantity of dissolved CsI in FLiNaK. Therefore, $P(\text{KI})$ was decided by the solubility of CsI into FLiNaK, and this solubility is constant for all samples. However the solubility of CsI was not well understood in this study.

In Figure 11, the CsI concentration dependence of $P(\text{K}^+)$. K is one of the constituent elements and most volatile species from the FLiNaK salt. The $P(\text{K}^+)$ did not change significantly with concentration of CsI. To expect what gas generated K^+ ion, the $P(\text{K}^+)$ was plotted with the vapor pressure of KF gas and KI gas from thermodynamic data. As seen in Figure 12, $P(\text{K}^+)$ corresponded with the vapor pressure of KI gas under 1073K for “CsI=50%”, “CsI=25%”, “CsI=10%”. At 1073K, these $P(\text{K}^+)$ were corresponding with the vapor pressure of KF gas. Therefore, it was expected that the K^+ ion was generated from KI, thereafter K^+ ion was generated by KF. For “CsI=1%”, CsI was not depleted over 1073K, therefore KI was not depleted and K^+ was generated from KI.

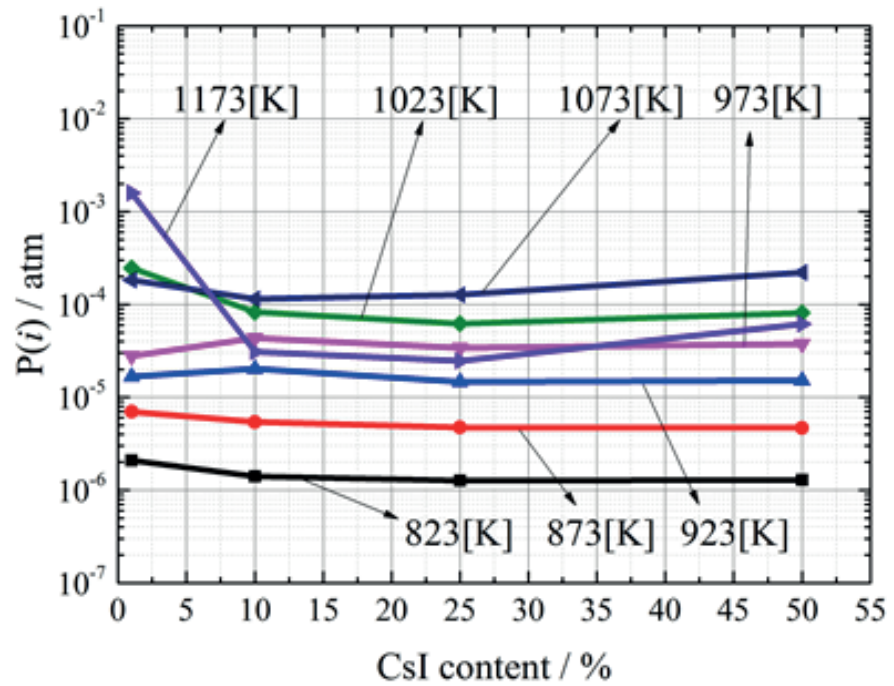


Figure 10: CsI concentration dependence of $P(i)$ for KI (focused on KI^+).

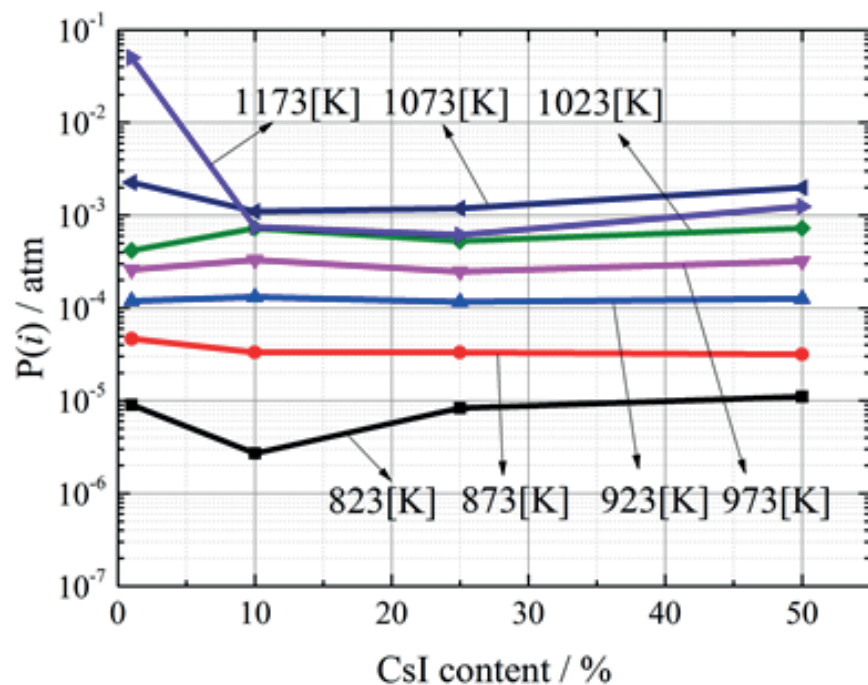


Figure 11: CsI concentration dependence of $P(i)$ for KI and KF (focused on K^+).

4. Conclusions

The released gases from pure FLiNaK were mainly KF, LiF and NaF. On the other hand, for FLiNaK with CsI, evaporated gases were expected to be KF, KI, CsI, $(CsI)_2$. It notes that the sample didn't include KI. It is expected that KI gas was generated by the reaction with FLiNaK

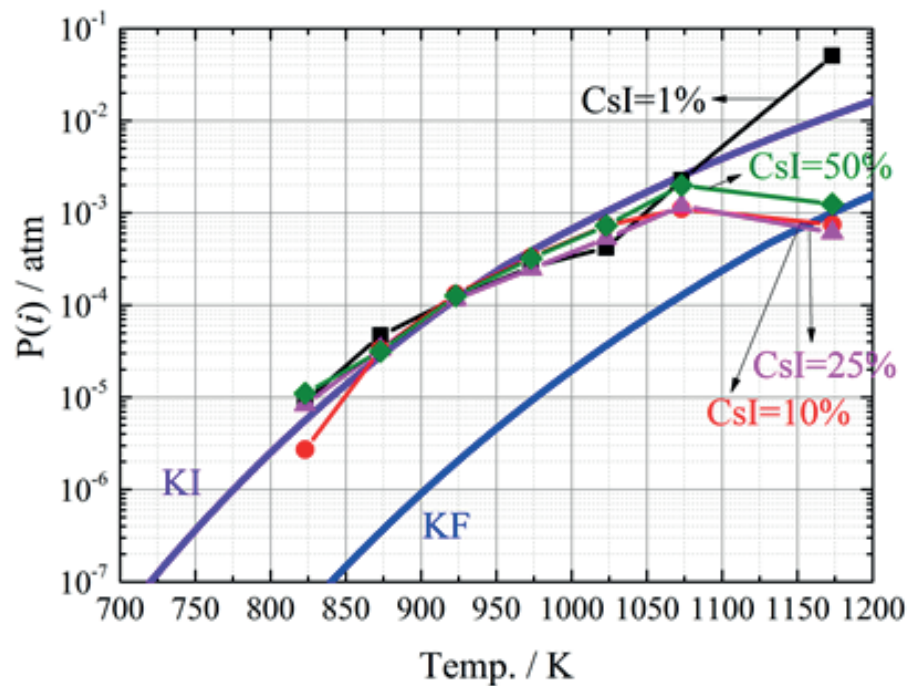


Figure 12: Comparing the thermodynamic database for KI and KF, and $P(i)$ of KI and KF (focused on K^+) for each samples.

and CsI. In the previous studies, when the severe accident in the LWR occurred, it is considered that I element will mostly combined with Cs element and release as CsI. Therefore, it is expected that the generation of KI gas is one of the characteristic points for SA in MSR. However, this mechanism was not well understood in this study.

The detected intensity for $P(K^+)$ might be generated by KI gas. This data is one reason for proving generation of KI. The $P(KI)$ of KI was no dependence on the CsI composition. It is considered that $P(KI)$ was decided by the solubility of CsI into FLiNaK, and this solubility is constant for all samples. However the solubility of CsI was not well understood in this study. Decision of this solubility needs further research or thermodynamic calculation.

The $P(CsI)$ and $P(I^+)$ are no dependence on the CsI composition for “CsI=10%”, “CsI=25%” and “CsI=50%”. It is expected that CsI could dissolve in FLiNaK completely under 10 mol%. Therefore $P(CsI)$ were corresponding with the vapor pressure of pure CsI. For “CsI=1%”, $P(CsI)$ and $P(I^+)$ were suppressed to about ten to the first ~ second power than the vapor pressure for pure CsI.

In the case of severe accident in MSR, fuel salt will be exposed to external environment. It is expected that the quantity of released CsI were limited more than in the case of LWR. The reason is considered that there is the margin of temperature about 100K than the case of LWR for the release quantity of CsI. Moreover it is expected that CsI in primary loop might be reduced by online-reprocessing continuously while MSR operates. Therefore it is expected that the quantity of CsI release will be very few than the case of LWR when the severe accident occurs in MSR. However, it notes that CsI is expected to release significantly at over 1073K.

Competing Interests

The authors declare no competing interests.

Acknowledgments

This study was partially supported by Chubu Electric Power Co., Inc.

References

- [1] The Generation IV International Forum, Technology Roadmap, https://www.gen-4.org/gif/jcms/c_9352/technology-roadmap.
- [2] Paul N. Haubenreich and J. R. Engel, "Experience with the Molten-Salt Reactor Experiment," *Nuclear Applications and Technology*, vol. 8, no. 2, pp. 118–136, 1970.
- [3] A. Nuttin, D. Heuer, A. Billebaud et al., "Potential of thorium molten salt reactors detailed calculations and concept evolution with a view to large scale energy production," *Progress in Nuclear Energy*, vol. 46, no. 1, pp. 77–99, 2005.
- [4] H. G. MacPherson, "The Molten Salt Reactor Adventure," *Nuclear Science and Engineering*, vol. 90, no. 4, pp. 374–380, 1985.
- [5] Report for the All Party Parliamentary Group on Thorium Energy Thorium-Fuelled Molten Salt Reactors, The Weinberg Foundation (2013).
- [6] C. Fiorina, M. Aufero, A. Cammi et al., "Investigation of the MSFR core physics and fuel cycle characteristics," *Progress in Nuclear Energy*, vol. 68, pp. 153–168, 2013.
- [7] D. Heuer, E. Merle-Lucotte, M. Allibert, M. Brovchenko, V. Ghetta, and P. Rubiolo, "Towards the thorium fuel cycle with molten salt fast reactors," *Annals of Nuclear Energy*, vol. 64, pp. 421–429, 2014.
- [8] Sylvie Delpech, "24 Molten salts for Nuclear Applications," in *Molten Salts Chemistry from Lab to Applications*, Lantelme Frédéric and Groult Henri, Eds., Elsevier, 2013.
- [9] S. Delpech, E. Merle-Lucotte, D. Heuer et al., "Reactor physic and reprocessing scheme for innovative molten salt reactor system," *Journal of Fluorine Chemistry*, vol. 130, no. 1, pp. 11–17xxx, 2009.
- [10] O. Beneš and R. J. M. Konings, "3.13 Molten salt reactor fuel and coolant," in *Comprehensive nuclear materials*, R. J. M. Konings, Ed., vol. 3, pp. 359–389, Elsevier, 2012.
- [11] V. Ignatiev, O. Feynberg, A. Merzlyakov et al., "Progress in development of MOSART concept with Th support," in *Proceedings of ICAPP, 12394*, Chicago, USA, 2012.
- [12] C. Yu, X. Li, X. Cai et al., "Minor actinide incineration and Th-U breeding in a small FLiNaK Molten Salt Fast Reactor," *Annals of Nuclear Energy*, vol. 99, pp. 335–344, 2017.
- [13] K. D. Carlson, *The Characterization of High Temperature Vapors*, Wiley, 1967, 115-129.
- [14] K. Murase, G.-Y. Adachi, M. Hashimoto, and H. Kudo, "Mass spectrometric investigation of the vapor over the LnCl₃-KCl equimolar melt (Ln=Nd, Er) at high temperatures," *Bulletin of the Chemical Society of Japan*, vol. 69, no. 2, pp. 353–357, 1996.
- [15] P. Mahadevan, G. D. Magnuson, J. K. Layton, and C. E. Carlston, "Secondary-electron emission from molybdenum due to positive and negative ions of atmospheric gases," *Physical Review A: Atomic, Molecular and Optical Physics*, vol. 140, no. 4A, pp. A1407–A1412, 1965.
- [16] J. B. Mann, *Recent Developments in Mass Spectroscopy*, University of Tokyo press, 1970.
- [17] U. Niemann, K. Hilpert, and M. Miller, "Study of the Heterocomplexes in the Vapor of the Na-Sn-Br-I System and Their Relevance for Metal Halide Lamps," *Journal of The Electrochemical Society*, vol. 141, no. 10, pp. 2774–2778, 1994.
- [18] I. Lisek, J. Kapala, and M. Miller, "Thermodynamic study of the CsCl-NdCl₃ system by Knudsen effusion mass spectrometry," *Journal of Alloys and Compounds*, vol. 278, no. 1-2, pp. 113–122, 1998.
- [19] M. Akiyama and K. Hayata, "Status of LWR Severe Accident Research," *Journal of the Atomic Energy Society of Japan / Atomic Energy Society of Japan*, vol. 35, no. 9, pp. 762–794, 1993.
- [20] C. D. Bowman et al., "Calendar," *Nuclear Instruments and Methods in Physics Research*, vol. 336, no. 1-2, p. 389, 1993.

- [21] C. D. Bowman, *Annu. Rev. Nucl. Part. Sci.*, vol. 48.
- [22] M. Hron, "Project SPHINX spent hot fuel incinerator by neutron flux (the development of a new reactor concept with liquid fuel based on molten fluorides)," *Progress in Nuclear Energy*, vol. 47, no. 1-4, pp. 347–353, 2005.
- [23] EURATOM MOST project, final report (2001).
- [24] V. Ignatiev, O. Feynberg, A. Myasnikov, and R. Zakirov, "Neutronic properties and possible fuel cycle of a molten salt transmuter," in *Proceedings of the Global 2003: Atoms for Prosperity: Updating Eisenhower's Global Vision for Nuclear Energy*, pp. 1873–1880, New Orleans, USA, November 2003.
- [25] V. Ignatiev, O. Feynberg et al., "Progress in development of Li, Be, Na/F molten salt actinide recycler and transmuter concept," in *Proceedings of ICAPP 2007*, pp. 3004–3013, Nice, France.
- [26] B. Becker, M. Fraton, and E. Greenspan, "2nd COE-INES International Symposium on Innovative Nuclear Energy Systems," in *Proceedings of the 2nd COE-INES International Symposium on Innovative Nuclear Energy Systems*, Yokohama, Japan, 2006.
- [27] T. Takizuka, T. Nishida, T. Sasa, H. Takada, and M. Mizumoto, "Studies on accelerator-driven transmutation at JAERI," in *Proceedings of 4th Intl. Information Exchange Mtg. on P-T, Mito 1113 September, OECD/NEA*, p. 161, Paris, 1996.
- [28] T. Mukaiyama, T. Takizuka, M. Mizumoto et al., "Review of research and development of accelerator-driven system in Japan for transmutation of long-lived nuclides," *Progress in Nuclear Energy*, vol. 38, no. 1-2, pp. 107–134, 2001, ADS special edition.
- [29] V. Berthou, I. Slessarev, and M. Salvatores, "Proposal of a molten-salt system for long-term energy production," in *Proceedings of the Workshop Proceedings of Advanced Reactors with Innovative Fuels*, Chester, UK, 2001.
- [30] V. Berthou, I. Slessarev, and M. Salvatores, "The TASSE concept (thorium based accelerator driven system with simplified fuel cycle for long term energy production)," in *Proceedings of the Proceeding of GLOBAL*, Paris, France, 2001.
- [31] I. Slessarev and P. Bokov, "On potential of thermo-nuclear fusion as a candidate for external neutron source in hybrid systems (applied to the "WISE" concept)," *Annals of Nuclear Energy*, vol. 30, no. 16, pp. 1691–1698, 2003.
- [32] A. Dudnikov, P. Alekseev, N. Kotkin, L. Menshikov, and S. Subbotin, "Proceeding of the 3rd International Conference on Accelerator-Driven Transmutation Technologies and Application, ADTTA99," in *Proceedings of the Proceeding of the 3rd International Conference on Accelerator-Driven Transmutation Technologies and Application, ADTTA99*, Prague, Czech, 1999.
- [33] P. N. Haubenreich and J. R. Engel, "Experience with the Molten-Salt Reactor Experiment," *Nucl. Appl. Technol.*, vol. 8, no. 2, pp. 118–136, 1970.
- [34] W. R. Grimes, "Molten Salt Reactor Chemistry," *Nucl. Appl. Technol.*, vol. 8, no. 2, pp. 137–155, 1970.
- [35] E. S. Bettis and R. C. Robertson, "The design and performance features of a single-fluid molten salt breeder reactor," *Nucl. Appl. Technol.*, vol. 8, no. 2, pp. 190–207, 1970.
- [36] M. E. Whatley, L. E. McNeese, W. L. Carter, L. M. Ferris, and E. L. Nicholson, "Engineering development of the MSBR fuel recycle," *Nucl. Appl. Technol.*, vol. 8, no. 2, pp. 170–178, 1970.
- [37] K. Furukawa, A. Lecocq, Y. Kato, and K. Mitachi, "Thorium Molten-Salt Nuclear Energy Synergetics," *Journal of Nuclear Science and Technology*, vol. 27, no. 12, pp. 1157–1178, 1990.
- [38] K. Furukawa, Y. Kato, and S. E. Chigrinov, "Plutonium (TRU) transmutation and ²³³U production by single-fluid type accelerator molten-salt breeder (AMSB)," in *Proceedings of the The international conference on accelerator-driven transmutation technologies and applications*, pp. 745–751, Las Vegas, Nevada (USA).
- [39] J. Vergnes and D. Lecarpentier, "The AMSTER concept (actinides molten salt transmuter)," *Nuclear Engineering and Design*, vol. 216, no. 1-3, pp. 43–67, 2002.
- [40] J. Vergnes and D. Lecarpentier, "The AMSTER concept (actinides molten salt transmuter)," *Nuclear Engineering and Design*, vol. 216, no. 1-3, pp. 43–67, 2002.
- [41] A. Mourogov and P. M. Bokov, "Potentialities of the fast spectrum molten salt reactor concept: REBUS-3700," *Energy Conversion and Management*, vol. 47, no. 17, pp. 2761–2771, 2006.
- [42] A. Mourogov and P. M. Bokov, "12th International Conference on Emerging Nuclear Energy Systems (ICECES' 2005)," in *Proceedings of the 12th International Conference on Emerging Nuclear Energy Systems (ICECES' 2005)*, Brussels, Belgique, 2005.
- [43] S. Delpech, E. Merle-Lucotte, D. Heuer et al., "Reactor physics and reprocessing scheme for innovative molten salt reactor system," *Journal of Fluorine Chemistry*, vol. 130, no. 1, pp. 11–17, 2009.
- [44] E. Merle-Lucotte, M. Allibert, M. Brovchenko, V. Ghetta, D. Heuer, and P. Rubiolo, "Preliminary design assessment of the molten salt fast reactor," in *Actes de la conférence European Nuclear Conference ENC2012*, Manchester, UK, 2012.
- [45] L. Mathieu, D. Heuer, E. Merle-Lucotte et al., "Possible configurations for the thorium molten salt reactor and advantages of the fast non moderated version," *Nuclear Science and Engineering*, vol. 161, no. 1, pp. 78–89, 2009.

- [46] L. Mathieu, D. Heuer, R. Brissot et al., “The thorium molten salt reactor: Moving on from the MSBR,” *Progress in Nuclear Energy*, vol. 48, no. 7, pp. 664–679, 2006.
- [47] E. Merle-Lucotte, D. Heuer, M. Allibert, V. Ghetta, and C. Le Brun, “Introduction to the Physics of Molten Salt Reactors,” in *Materials Issues for Generation IV Systems*, NATO Science for Peace and Security Series B: Physics and Biophysics, pp. 501–521, Springer Netherlands, Dordrecht, 2008.
- [48] J. B. Mann, “Ionization cross sections of the elements calculated from mean-square radii of atomic orbitals,” *The Journal of Chemical Physics*, vol. 46, no. 5, pp. 1646–1651, 1967.